Probing nuclear structure of ^{124}Xe

B. Saha,[1] A. Dewald,[1] O. Möller,[1] R. Peusquens,[1] K. Jessen,[1] A. Fitzler,[1] T. Klug,[1] D. Tonev,[1] P. von Brentano,[1] J. Jolie,[1] B. J. P. Gall,[2] and P. Petkov[1,3]

[1]*Institut für Kernphysik der Universität zu Köln, 50937 Köln, Germany*

[2]*IReS, UMR7500IN2P3-CNRS, Université Louis Pasteur, Strasbourg, France*

[3]*Bulgarian Academy of Sciences, Institute for Nuclear Research and Nuclear Energy, 1784 Sofia, Bulgaria*

(Received 2 June 2004; published 28 September 2004)

Excited states in ^{124}Xe were populated in the fusion-evaporation reaction ^{110}Pd(^{18}O,4n)^{124}Xe at a beam energy of 80 MeV. A recoil distance measurement using the Euroball spectrometer in Strasbourg and the Cologne plunger was performed. Altogether 19 lifetimes of excited states in six different bands were determined using gated spectra only, in order to avoid problems related to feeding. The measured $B(E2)$ values were used to derive the nuclear deformation of ^{124}Xe and the interaction of the ground state band with two s bands. Two sd-IBM-1 calculations with two Hamiltonians of different complexities were performed, which show a good agreement with the measured $B(E2)$ values in the ground state band and the quasi-γ band. The deduced $B(M1)$ values for the regular $M1$ band show the behavior expected for magnetic rotation. However, it is also shown that these experimental $B(M1)$ values can be described on the basis of a rotational band as well.

DOI: 10.1103/PhysRevC.70.034313 PACS number(s): 21.10.Tg, 21.60.Ev, 23.20.Lv, 27.60.+j

I. INTRODUCTION

The nucleus ^{124}Xe is known to be γ soft, with a moderate β deformation. The picture of γ softness and triaxiality has been studied in details in Ref. [1]. In a recent work by Werner *et al.* [2] calculations performed in the framework of the *sd* version of the interacting boson model [3,4] revealed typical features of the $O(6)$ dynamical limit, as well as signatures showing contributions of the $U(5)$ symmetry in ^{124}Xe. At higher excitation energies of about 3.5 MeV $\nu(h_{11/2})^2$ and $\pi(h_{11/2})^2$ quasiparticle excitations occur and two s bands built on these states can be followed up to spins $I^\pi = 24^+$ and 16^+, respectively. A systematics of such s bands in the Xe-Ba-Ce region was investigated in Refs. [5,6]. Another interesting feature of ^{124}Xe is the existence of a regular $M1$ band [7], which has been considered to be a promising candidate for magnetic rotation (see Fig. 1). The theoretical description of magnetic rotation is given in the framework of the tilted axis cranking (TAC) model developed by Frauendorf [8]. Experimentally it was first established in the neutron deficient Pb isotopes [9,10]. In several nuclei of the $A \approx 130$ mass region $M1$ bands like those observed in the $A \approx 200$ mass region are known, but here the underlying structure is still under discussion, e.g., in ^{124}Xe and ^{128}Ba. One signature of magnetic rotation is the decrease of the $B(M1)$ values with increasing spin. Consequently, absolute reduced transition probabilities are crucial experimental observables for testing the structure of magnetic rotation as well as other nuclear excitations, which have been observed in ^{124}Xe. In this work we will present the results of a recoil distance measurement (RDM) performed to determine lifetimes of excited states in ^{124}Xe.

II. EXPERIMENTAL DETAILS AND DATA ANALYSIS

The experiment for ^{124}Xe was performed with the Euroball IV [11] spectrometer using the Cologne coincidence plunger device at the Vivitron accelerator of the IReS in Strasbourg. Excited states in ^{124}Xe were populated by the ^{110}Pd(^{18}O,4n) reaction at a beam energy of 80 MeV. The target consisted of a 1.1 mg/cm^2 thick self-supporting ^{110}Pb foil. The recoils, leaving the target with a velocity of 0.98% of the velocity of light, c, were stopped in a 6.0 mg/cm^2 Au foil. During the experiment, data were taken at 21 different target-to-stopper distances ranging from electrical contact to 2000 μm. Figure 2 shows examples of gated spectra for different target-to-stopper distances.

The used plunger apparatus is designed especially for $\gamma\gamma$ coincidence recoil distance measurements. It is equipped with a feedback system in order to compensate for slow variations of the target-to-stopper distance, caused, e.g., by the heating of the system by the beam.

The accuracy of the relative distances is better than 0.1 μm in the range from electrical contact of the target and stopper foils to 20 μm and better than 1 μm in the range 20–2000 μm. Further details are given in Ref. [12].

For the data analysis the differential decay curve method (DDCM) [13] was used. According to this method for each flight time t a lifetime value τ for the level of interest is calculated from quantities which are obtained directly from the measured data. The DDCM can be applied for singles as well as for $\gamma\gamma$ coincidence data. In the case where $\gamma\gamma$ coincidences are measured in a RDM experiment, the lifetime can be determined from the following equation:

$$\tau(x) = \frac{\{C_S A_U\}(x) - \alpha \cdot \{C_S B_U\}(x)}{d/dx\{C_S A_S\}(x)} \frac{1}{v}, \tag{1}$$

where

$$\alpha = \frac{\{C_S A_U\} + \{C_S A_S\}}{\{C_S B_U\} + \{C_S B_S\}},$$

and v is the recoil velocity. The quantities in braces are the

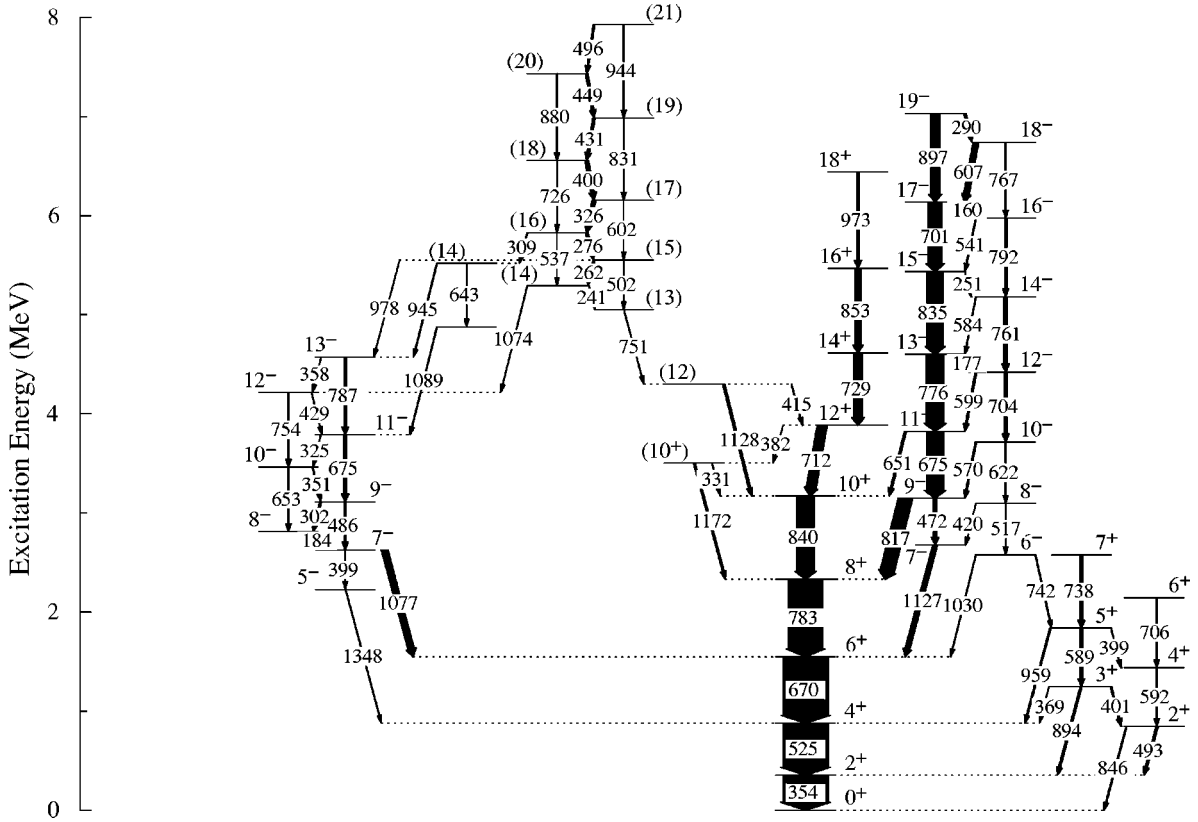

FIG. 1. Partial level scheme of ^{124}Xe (see Ref. [7]).

numbers of events corresponding to the detection of the Doppler-shifted (S) or unshifted (U) components of the γ-ray transitions involved in the analysis. Transition A depopulates the level of interest, whose lifetime has to be determined and which is directly fed by the transition B. The gate is set on the S component of transition C that lies higher in a cascade above the level of interest. In the case of a gate set on a direct feeder, Eq. (1) reduces to

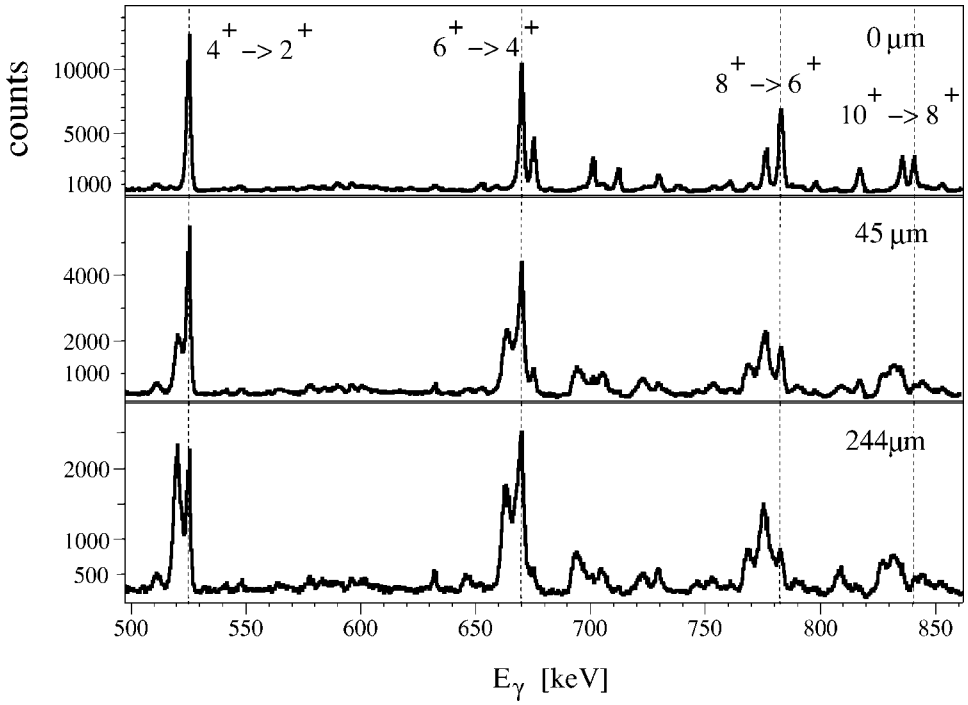

FIG. 2. Gated spectra for ^{124}Xe taken at the indicated target-to-stopper distances from an angle θ=156.1° with respect to the beam axis. The vertical lines show the positions of the unshifted peaks.

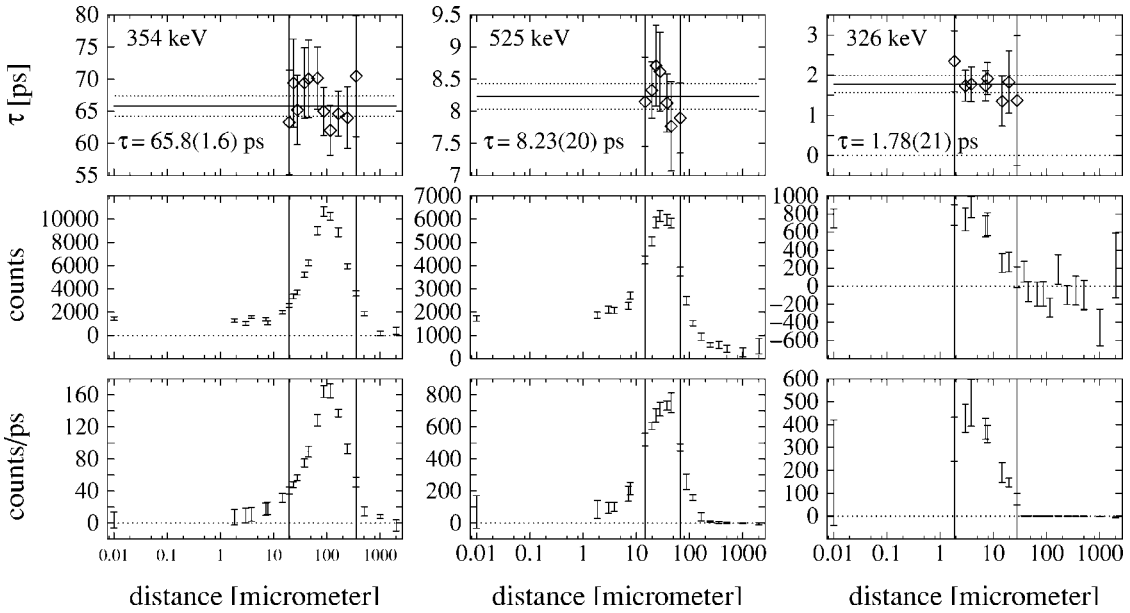

FIG. 3. τ curves $\tau(x)$ given for the 354, 525 keV ground state band transitions and for the 326 keV transition of the $M1$ band (upper panels). Also given are the quantities $\{B_S A_U\}(x)$ and $d/dx\{B_S A_S\}(x)$ (middle and lower panels, respectively) used to determine the $\tau(x)$ values (see text).

$$\tau(x) = \frac{\{B_S A_U\}(x)}{d/dx\{B_S A_S\}(x)} \frac{1}{v}. \tag{2}$$

Since the lifetimes τ are calculated for every flight time $t = x/v$ one obtains a function $\tau(t)$ or $\tau(x)$, i.e., the so-called τ curve which is expected to be a constant. Deviations from a constant behavior indicate the presence of systematic errors. Examples for τ curves for the 2^+ and 4^+ states of the ground state band and for the spin 16 state of the $M1$ band are given in Fig. 3 together with the quantities $\{B_S A_U\}(x)$ and $d/dx\{B_S A_S\}(x)$ which were used to calculate the corresponding $\tau(x)$ values. Further details of the DDCM can be found in Refs. [13,14].

For the data analysis, detectors positioned at almost identical angles θ with respect to the beam axis were grouped into rings. Consequently the spectra measured with detectors belonging to one ring show the same Doppler shifts. In Table I, the assignments of the detectors to eight rings are given.

For each target-to-stopper distance the data were sorted into $\gamma\gamma$ matrices corresponding to all possible ring combinations. Lifetimes τ_i determined using different matrices are statistically independent and allow for consistency checks. The mean value of the corresponding independent lifetimes τ_i was finally taken as the adopted level lifetime τ. Due to the occurrence of doublets even in gated spectra, not all possible gates and matrices generated from the different ring combinations were used for the lifetime analysis. Table II gives the employed gates and rings for all determined lifetimes.

Effects due to the deorientation of the recoiling nuclei in vacuum do not enter the DDCM analysis when gates are set on the S components (see Table II) of feeding transitions [15], so-called "gates from above." In the case of a gate set on the U component of a depopulating transition ("gate from below") the deorientation effect has to be considered, but is of importance only for spins $I < 6\hbar$ [15,16].

Furthermore, the effects of the velocity distribution of the recoiling nuclei and the Doppler-shift attenuation occurring during the slowing down in the stopper were taken into account. For this purpose gated spectra were simulated using all known parameters of the kinematics of the recoiling nuclei, material properties of the target and stopper foils and geometrical and spectroscopic features of the Euroball spectrometer [16,17]. The simulated spectra for a hypothetical band chosen such, to describe in a realistic way the experimental case, were analyzed in the same way as the experimental spectra. For the hypothetical band level lifetimes between 0.34 and 2.63 ps and transition energies between 600 and 1100 keV were chosen. Gated spectra were simulated for different rings in backward and forward directions and for longer and shorter feeding times. By comparing the derived lifetime values with the values used for the simula-

TABLE I. Angles of the 239 detectors of the Euroball spectrometer with respect to the beam axis and their assignment into rings.

Ring	Mean angle θ (°)	Number of detectors	Type
0	156.1±5.4	35	Cluster
1	137.1±5.4	35	Cluster
2	129.7±5.4	35	Cluster
3	103.3±4.2	52	Clover
4	76.5±4.4	52	Clover
5	52.23±0	15	Tapered
6	34.6±0	10	Tapered
7	15.45±0	5	Tapered

TABLE II. Rings used for gating and rings, from which the gated spectra were taken (gated rings) to detemine the intensities of interest according to Eq. (1). In column 5 the transition energy on which the gate was set is presented. *S* and *U* indicate if the gate was set on the shifted or unshifted component of the transition, respectively.

E_{lev} (keV)	I^{π}	Rings for gating	Gated rings	$E_{\gamma}^{U/S}$ (keV) of the gate
354	2^+	0,1,2,5,6,7	0,1,2,5,6,7	525^S
879	4^+	0,1,2	0,1,2,6,7	670^S
1549	6^+	0,1,2,5,6,7	0,1,2,5,6,7	853^S, 730^S, 712^S
2331	8^+	0,1,2,5,6,7	0,1,2,5,6,7	853^S, 730^S, 712^S, 973^S
3172	10^+	0,1,2,5,6,7	0,1,2,5,6,7	853^S
3883	12^+	0,1,2,5,6,7	0,1,5,6,7	730^S
4299	12^+	0,1,2	0	815^S
5552.7	(15)	0,1,2,5,6,7	0,1	276^S
5828.3	(16)	0,1,2,5,6,7	0,1,7	326^S
6154.8	(17)	0,1,2,5,6,7	0,1,6,7	400^S
6554.6	(18)	0,1,2,5,6,7	0,1,2,5	431^S
846.6	2^+	0,1,2,5,6,7	0,1,2,5,6	592^S
1247.7	3^+	0,1,2,5,6,7	0,1,2,5	738^S
1836.9	5^+	0,1,2,5,6,7	0,1,2,5	738^S
3147.8	9^-	5,6,7	0,1,2,5	675^S
3822.6	11^-	0,1,2	0,1,2	675^U
4598.8	13^-	5,6,7	0,1,2	776^U
5434.1	15^-	5,6,7	0,1,2	835^U
6134.9	17^-	0,1,2,5,6,7	0,1,2,5,6,7	897^S
2625.7	7^-	0,1,2,5,6,7	0,1,2,5,6	1077^U

tions, correction factors were extracted. The correction factor as a function of the corresponding lifetime τ can be described with the function $c(\tau)=1+a\cdot\exp[-b\cdot\tau(\mathrm{ps})]$, using the parameters $a=0.90(16)$ and $b=2.01(29)\mathrm{ps}^{-1}$ (see Fig. 4).

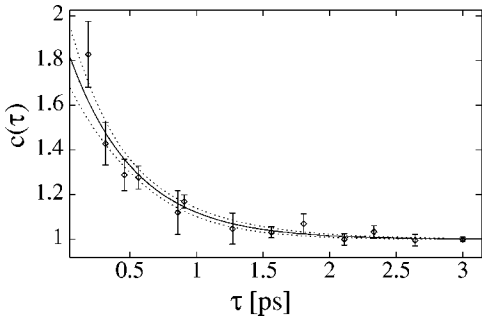

FIG. 4. Correction factor $c(\tau)$ as a function of the corresponding lifetime to correct the effects of the velocity distribution of the recoiling nuclei and the Doppler-shift attenuation occurring during the slowing down in the stopper and target. Here τ are the lifetime values obtained in the analysis without considering the slowing down time of the recoils.

Ten lifetimes below 3 ps were corrected for this effect as indicated in Table III.

Overall 19 lifetimes were determined, six in the ground state band up to the 12^+ state, five in the yrast negative parity band up to the 17^- state, three of the γ-band, one of the "negative parity" band, and four in the $M1$ band for states with spins from 15 to 18 $\hbar$. Table III shows all adopted lifetime values τ and the corresponding transition probabilities. Mixing ratios δ used for the calculation of the transition probabilities in the $M1$ band were taken from Ref. [7] and for the quasi-γ band from Ref. [2]. In columns 6 and 7 of Table III the lifetimes from two previous works [18,19] are given for comparison. Both works are based on the same singles data set, but use different analyzing techniques and feeding assumptions. The deorientation effect for the 2_1^+ state was only taken into account in Ref. [19], which explains the large difference of $\tau(2_1^+)=48(3)$ and 60(5) ps from Refs. [18,19], respectively. The transition probabilities within the ground state band and the $M1$ band will be discussed in the following sections.

III. $B(E2;0^+\rightarrow 2^+)$ SYSTEMATICS AND GROUND STATE DEFORMATIONS

Much work has been devoted to describe the behavior of nuclear deformation over a wide mass range. For instance, Casten successfully parameterized the $B(E2;0^+\rightarrow 2^+)$ values in the $A=150$ and $A=100$ mass region using the product of the proton and neutron boson numbers $N_{\pi}^{B}\cdot N_{\nu}^{B}$ [20]. In the $A=130$ mass region the picture presented by the experimental values was not clear since contradictory lifetimes of the 2^+ level were published for several nuclei. The improved techniques of lifetime measurements, in particular the use of $\gamma\gamma$ coincidence data and the DDCM analysis [13], which became available in the last years, helped a lot to improve the quality of the experimental data and correct wrong results. Now the resulting $B(E2)$ systematics (Fig. 5) shows a very regular behavior, which allows a quantitative description of the observed $B(E2;0^+\rightarrow 2^+)$ values for many nuclei of this region by the following relation [21]:

$$B(E2;0^+\rightarrow 2^+)=\alpha\cdot N_{\pi}\cdot N_{\nu}+B(E2;0^+\rightarrow 2^+)_{^{124}Sn}, \quad (3)$$

where N_{π} and N_{ν} are the number of proton particles and neutron holes counted from the nearest closed shell, and α is a free parameter. The value $\alpha=0.0215$ $\mathrm{e}^2\mathrm{b}^2$ was obtained by fitting the experimental data. This systematics of $B(E2;0^+\rightarrow 2^+)$ values reveals a linear dependence on the product $N_{\pi}\cdot N_{\nu}$ for $N_{\pi}<8$ and for $N_{\pi}=10$, $N_{\nu}\leqslant 10$ of the nuclear deformation in the $A=130$ mass region. Beyond these values enhanced deformation driving forces become apparent, e.g., in the case of the occupation of the $1/2[541]$ Nilsson orbital by two neutrons.

The measured lifetime $\tau=67.5(17)$ ps of the first 2^+ level of ^{124}Xe gives a $B(E2;0^+\rightarrow 2^+)$ value of 1.07(6) $\mathrm{e}^2\mathrm{b}^2$ which is close to the value given by Eq. (3).

The 2_1^+ lifetime from this work is a bit longer than $\tau=60(3)$ps obtained in a previous singles RDM experiment [19]. Comparing the deformation $\beta=0.218$ of ^{124}Xe, deduced

TABLE III. Lifetime results for ^{124}Xe. The lifetime values τ along with the energies of the levels, deexciting γ ray energies, and initial and final spins are given. Futhermore the reduced transition probabilities $B(\sigma L)$ are given in $e^L\mathrm{fm}^{2L}$ for electric transitions and in $\mu_N^2\mathrm{fm}^{2L-2}$ for magnetic ones. In columns 6 and 7 lifetimes from previous works (see Refs. [18,19]) are presented.

E_{lev} (keV)	E_γ (keV)	I_i^π	I_f^π	σL	τ [a] (ps)	τ [b] (ps)	τ (ps)	τ adopted (ps)	$B(\sigma L)$
354	354	2^+	0^+	$E2$	48(3)	60(5)	67.5(17)	67.5(17)	$2121.5^{+54.8}_{-52.1}$
879	525	4^+	2^+	$E2$	5.1(6)	5.6(6)	8.19(23)	8.19(23)	$2487.0^{+71.9}_{-67.9}$
1549	670	6^+	4^+	$E2$	1.4(5)	1.1(4)	1.82(17)	1.86(16)[c]	3251^{+306}_{-258}
2331	783	8^+	6^+	$E2$	1.5(6)	0.5(12)	1.03(39)	1.15(35)[c]	2415^{+1060}_{-563}
3172	840	10^+	8^+	$E2$	2.2(5)	$\leqslant$1.4	2.49(33)	2.51(32)[c]	778.5^{+114}_{-88}
3883	712	12^+	10^+	$E2$	<4		2.13(37)	2.16(36)[c]	2024^{+628}_{-449}
	381	12^+	10^+	$E2$					926^{+297}_{-212}
4299	1128	12^+	10^+	$E2$			>2.5	>2.5	<102
5552.7	261.6	(15)	(14)	$M1$			0.89(8)	1.02(8)[c]	$1.44^{+0.28}_{-0.24}$
	261.6	(15)	(14)	$E2$					5908^{+1136}_{-972}
	501	(15)	(13)	$E2$					1018^{+225}_{-192}
5828.3	275.9	(16)	(15)	$M1$			1.84(13)	1.88(12)[c]	$1.02^{+0.18}_{-0.16}$
	275.9	(16)	(15)	$E2$					3738^{+653}_{-575}
	537	(16)	(14)	$E2$					586^{+123}_{-109}
6154.8	326.5	(17)	(16)	$M1$			1.75(8)	1.80(8)[c]	$0.75^{+0.11}_{-0.10}$
	326.5	(17)	(16)	$E2$					2003^{+304}_{-278}
	602	(17)	(15)	$E2$					708^{+141}_{-129}
6554.6	400	(18)	(17)	$M1$			0.40(8)	0.56(9)[c]	$1.33^{+0.41}_{-0.30}$
	400	(18)	(17)	$E2$					2360^{+734}_{-531}
	726	(18)	(16)	$E2$					893^{+327}_{-236}
846.6	493.0	2^+	2^+	$M1$	10(2)		17.8(30)	17.8(30)	$3.1^{+1.7}_{-4.2}\times10^{-4}$
	493.0	2^+	2^+	$E2$					1143^{+2144}_{-454}
	846.6	2^+	0^+	$E2$					$28.1^{+9.4}_{-6.7}$
1247.7	401.1	3^+	2^+	$M1$	9(2)		9.0(10)	9.0(10)	$1.4^{+4.7}_{-1.1}\times10^{-4}$
	401.1	3^+	2^+	$E2$					3024^{+552}_{-512}
	893	3^+	2^+	$M1$					$4.0^{+1.5}_{-1.3}\times10^{-4}$
	893	3^+	2^+	$E2$					$83.6^{+16.2}_{-14.6}$
	368.8	3^+	4^+	$M1$					$5.9^{+2.8}_{-2.2}\times10^{-4}$
	368.8	3^+	4^+	$E2$					925^{+206}_{-191}
1836.9	589.2	5^+	3^+	$E2$	4.5(6)		5.75(25)	5.75(25)	1379^{+187}_{-186}
	399	5^+	4^+	$M1$					$5.4^{+5.5}_{-3.4}\times10^{-4}$
	399	5^+	4^+	$E2$					1308(251)
	958.1	5^+	4^+	$M1$					$6.1^{+2.2}_{-1.8}\times10^{-4}$
	958.1	5^+	4^+	$E2$					$26.7^{+5.5}_{-5.2}$
3147.8	816.7	9^-	8^+	$E1$	5(1)		5.23(71)	5.23(71)	$17.0^{+4.6}_{-3.5}\times10^{-5}$
3822.6	674.8	11^-	9^-	$E2$	1.2(8)		3.18(9)	3.18(9)	1689^{+224}_{-211}
4598.8	775.9	13^-	11^-	$E2$	2.5(15)		1.56(8)	1.62(8)[c]	1776^{+279}_{-253}
5434.1	835.3	15^-	13^-	$E2$	4.2(12)		1.99(11)	2.02(11)[c]	957^{+156}_{-140}
6134.9	701.0	17^-	15^-	$E2$			4.25(21)	4.25(21)	1085^{+170}_{-154}
2625.7	1077	7^-	6^+	$E1$	148(15)		98.7(96)	98.7(96)	$4.9^{+1.1}_{-0.9}\times10^{-6}$

[a]See Ref. [18].
[b]See Ref. [19].
[c]Lifetimes corrected due to the slowing down of the recoils in the target and stopper foils.

with the new $B(E2)$ value, with its Xe neighbors it stays close to the value of ^{126}Xe (β=0.216) whereas the deformation of β=0.252 determined for ^{122}Xe is considerably larger. In Fig. 6 the Q_t values of the ground state band (GSB) in ^{124}Xe are shown together with those of ^{126,122}Xe. The experimental values are compared with theoretical values of the ion bombardment and annealing limits $U(5)$ and $O(6)$ and the rotor model. The best agreement is obtained for the $O(6)$

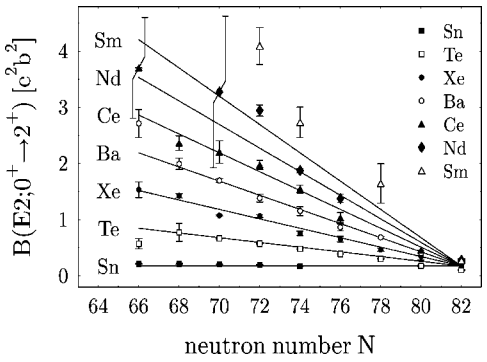

FIG. 5. $B(E2;0^+\rightarrow 2^+)$ values plotted vs the neutron number N. The value of ^{124}Xe for $N=70$ is taken from this work. Other data shown are taken from Ref. [12] and references given therein.

limit although the experimental $Q_t(4^+\rightarrow 2^+)$ values deviate from the calculated ones. This is especially apparent in ^{124}Xe where the deviation from $O(6)$ is 8%. From the reliable value of the 4^+ level it follows that the deviation is a real effect. Although we deal with a dominant collective structure, shell effects might possibly underlie this reduction of $E2$ strength. The strong reduction of the $Q_t(10^+\rightarrow 8^+)$ value by 42%

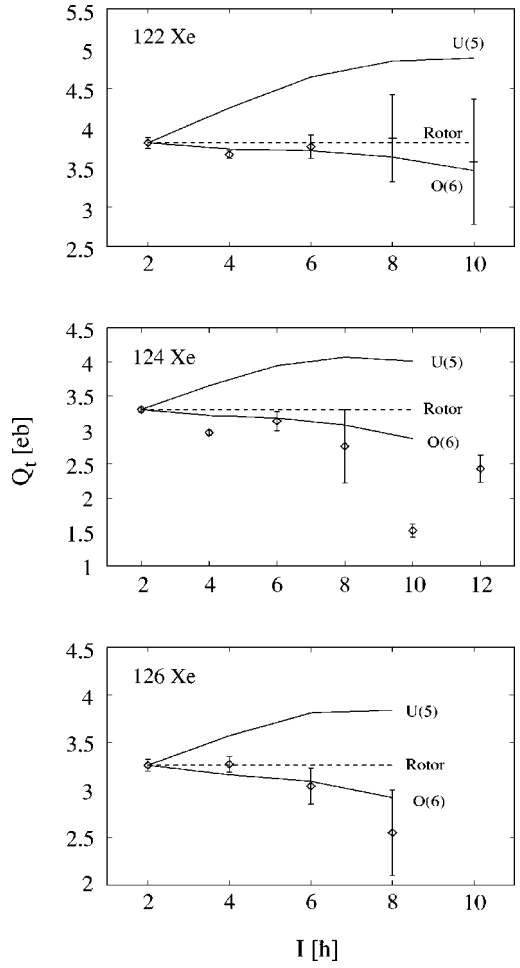

FIG. 6. Q_t values of ^{124}Xe and its neighbors ^{122}Xe and ^{126}Xe compared to the $U(5)$ and $O(6)$ symmetries of the IBM.

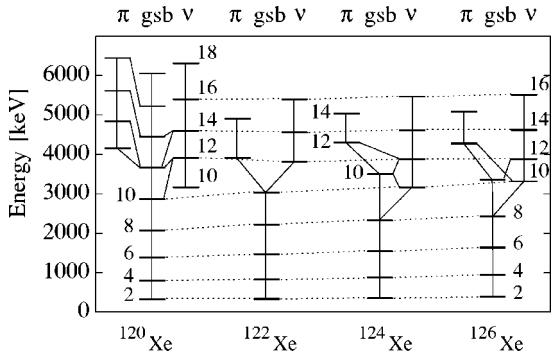

FIG. 7. Comparison of the level energies in ^{120,122,124,126}Xe for the GSB, $\pi(h_{11/2})$ band, and the $\nu(h_{11/2})$ band.

indicates the crossing of the ground state band with the first s band. This is a particularly beautiful case of band crossing, which will be discussed in more detail in the following section.

IV. GSB COLLECTIVITY AND BAND MIXING IN ^{124}Xe

The crossing of the ground state band with two s bands has been observed in many nuclei in the $A=130$ mass region at spin 10 [5,6]. In cases where sufficient spectroscopic data for the crossing region are available, a level mixing calculation can deliver interesting information on the interaction strength of the different nuclear structures which are represented by the observed bands.

Such calculations had been performed, e.g., for ^{128}Ba [12,22], ^{130}Ba [12], and ^{124}Xe [23]. In the case of ^{130}Ba, also absolute transition probabilities were considered in the calculations. Since for ^{124}Xe lifetimes of states in the crossing region were measured, we performed a three band mixing calculation. The strongly reduced transition probability for the $(10^+\rightarrow 8^+)$ transition (see Fig. 6) already indicates a considerable structural change of the ground state band at the 10^+ state and weak mixing. Unfortunately only two 10^+ states at 3172 and 3503 keV are known. A third 10^+ state has not been identified so far. The relatively large $Q_t(12^+\rightarrow 10^+)$ value indicates that the structure of the 10^+ state is similar to that of the 12^+ state, which is assumed to belong to the $\nu(h_{11/2})^2$ s band [5,6]. As a consequence, the second 10^+ state appears to be the perturbed state of the ground state band heritage. It is amazing that the relative energies of the $\nu(h_{11/2})^2$ s band are constant within a few kilo-electron-volts in the nuclei ^{126,124,122,120}Xe as shown in Fig. 7.

This indicates that the energy of the unperturbed $\nu(h_{11/2})^2$ 10^+ state in ^{124}Xe can reliably be estimated. Using the lifetimes, $E2$ branching ratios, and level energies, a mixing calculation was performed, which reproduces the experimental information very well. In Fig. 8 the relevant part of the level scheme is presented together with the experimental and calculated absolute transition probabilities. For the 10^+ states interaction strengths of $V_{g\nu}=160$ keV, $V_{g\pi}=10$ keV, and $V_{\nu\pi}=50$ keV were derived. The latter two values were obtained on the basis of estimated level energies. Table IV shows the mixing amplitudes $\langle\mu|n\rangle$ and the unperturbed and

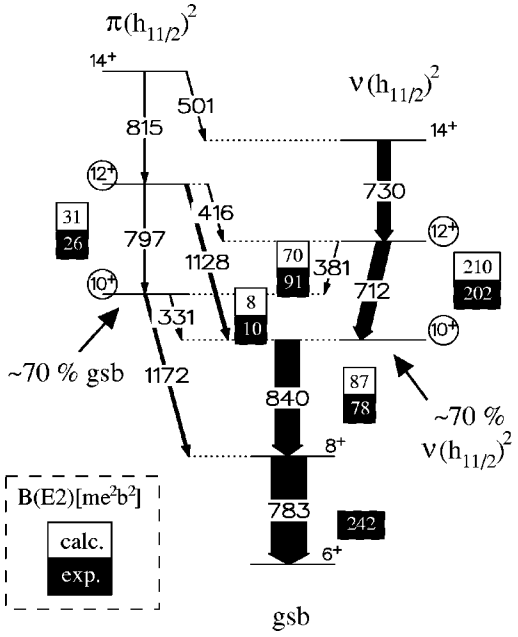

FIG. 8. Comparison of absolute $B(E2)$ values (black boxes) with corresponding values from the three level mixing calculation (white boxes). The values are given in me^2b^2.

perturbed level energies of the 10^+ states E^0_μ and E_n, respectively. Although the agreement between experiment and calculation is good an open question remains: Why the $\pi(h_{11/2})^2$ 10^+ state has not been observed? The level energy of this state in ^{124}Xe was extrapolated from higher spin states of the corresponding band to be $E=3800$ keV. It has not been observed in one of the neighboring Xe nuclei (cf. Fig. 7). This holds for ^{120}Xe as well, where many states of the ground state band and both *s* bands were observed, but not the $\pi(h_{11/2})^2$ 10^+ state. A possible explanation might be that the excitation energy of this state is quite high and that a small $(12^+ \rightarrow 10^+)$ transition energy leads to a weak transition.

V. *M*1 BAND IN ^{124}Xe

In recent years cascades of enhanced magnetic dipole *M*1 transitions have been observed in the neutron-deficient Pb nuclei [24,25]. A number of similar bands were also found in the $A\approx 110$ and $A\approx 140$ regions. The properties of these bands have been successfully described by the TAC model developed by Frauendorf [8] as well as the semiclassical model introduced by Macchiavelli [26,27]. In these models the band-head configuration in the Pb isotopes arises from a perpendicular coupling of the angular momenta of high-*K* protons and high-*j* neutron holes. Angular momentum in these bands is gained by simultaneous step-by-step reorientation of the proton-particle and the neutron-hole angular momenta into the direction of the total angular momentum *I*. One can picture this as the closing of the blades of shear, leading to the name "shears bands" [25]. The characteristic feature of the shears mechanism is a decrease of $B(M1)$ values for the dipole transitions with increasing angular momentum, since the $B(M1)$ values are proportional to the components of the magnetic moments perpendicular to the total angular momentum. Recent lifetime measurements in the light Pb isotopes [9,10] had confirmed this behavior experimentally.

TABLE IV. Mixing amplitudes $\langle \mu | n \rangle$ and their squares (in brackets) for the 10^+ state, where $\mu=\pi, \mathrm{GSB}, \nu$ denotes the unperturbed states and $n=1,2,3$ the perturbed ones. Further the corresponding level energies E^0_μ and E_n are presented. The interaction strengths are $V_{g\nu}=160$ keV, $V_{g\pi}=10$ keV, and $V_{\nu\pi}=50$ keV.

n	1	2	3	E^0_μ
μ				(keV)
π	−0.056(0.003)	0.127(0.016)	0.990(0.981)	3793
GSB	−0.578(0.335)	−0.813(0.660)	0.072(0.005)	3395
ν	0.814(0.662)	−0.569(0.323)	0.119(0.014)	3288
E_n (keV)	3171	3505	3800[a]	

[a]Extrapolated data (see text).

In many nuclei of the $A=130$ mass region, bands with strong *M*1 transitions and weak crossover *E*2 transitions have also been observed. Therefore, the question arises if these bands can be considered as shears bands. This was discussed in several papers [7,28]. Whereas the nuclei in the Pb region are almost spherical, the nuclei in the $A=130$ region are deformed ($\beta\approx 0.2$), e.g., Ba and Xe nuclei. Therefore, the collective rotation perpendicular to the symmetry axis, which can almost be neglected in Pb nuclei, is expected to have a larger influence in nuclei of the $A=130$ mass region. Especially in the case of ^{128}Ba intense experimental and theoretical studies had been devoted to the *M*1 band [28,29]. On the basis of branching ratios, mixing ratios δ, and lifetimes it had been revealed, that this band can be described as a rotational band, built on the four quasiparticle excitation $\pi(h_{11/2}d_{5/2}) \otimes \nu(h_{11/2}g_{7/2})$ with an effective *K* value of about $9\hbar$ [28]. The most important signature for excluding a shears band structure in the case of the *M*1 band in ^{128}Ba are $B(M1)$ values which increase with the spins. This increase is most pronounced for the low spin part of the band. The investigation of the *M*1 band in ^{124}Xe, which is very similar to the one in ^{128}Ba, was a major subject of the Euroball lifetime experiment performed at Strasbourg and described in this work. The band in ^{124}Xe also shows strong *M*1 transitions and weak crossover *E*2 transitions, but also differences have been observed. The signs of the δ values are negative in ^{124}Xe and positive in ^{128}Ba. Unfortunately the parity of the *M*1 band in ^{124}Xe is not fully established. So far we determined the lifetimes of the four lowest lying states in the *M*1 band.

The deduced *E*2 and *M*1 transition probabilities are shown in Fig. 9. It is evident that the $B(M1)$ transition probabilities are decreasing with increasing spin, which is the expected behavior for a shears band and is in contrast to the corresponding values in ^{128}Ba. In order to check whether a rotational band built on a four quasiparticle state is also compatible with the observed decreasing $B(M1)$ values we used the relation [30]

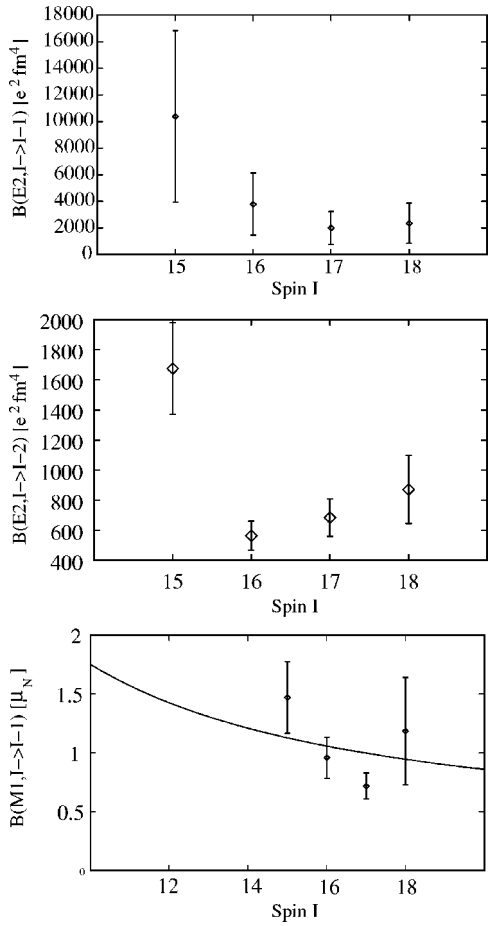

FIG. 9. $E2$ and $M1$ transition probabilities of the $M1$ band of ^{124}Xe. The solid line in the bottom part of the figure represents a semiclassical calculation using Eq. (4).

$$B(M1) = \frac{3K^2}{8\pi}\left\{\tilde{g}_2\left[\sqrt{1-\left(\frac{K}{I}\right)^2} - \frac{i_2}{I}\right] - \tilde{g}_1\frac{i_1}{I}\right\}^2 \qquad (4)$$

for the four quasiparticle structure $\pi(h_{11/2})^2 \otimes \nu(h_{11/2}g_{7/2})$. The proton part $\pi(h_{11/2})^2$ as well as the neutron part $\nu(h_{11/2}g_{7/2})$ were observed in the low spin spectrum of ^{124}Xe, and the $M1$ band decays to both structures. It was assumed that the two protons and the two neutrons align pairwise to a common proton and neutron spin $j_1 = 10\hbar$ and $j_2 = 8\hbar$, respectively, which couple with the collective spin R to the total spin I. The quantities $i_1 \approx 10$ and $i_2 \approx 0$ used in Eq. (4) are the alignments of j_1 and j_2, respectively. The g factors of the proton and neutron contributions $\tilde{g}_1$ and $\tilde{g}_2$ were calculated using the g factors of the involved single particle orbitals given in Ref. [31]. The value of K was varied to obtain the best agreement with the experimental data. The result of the calculation is shown as a solid line in the lower part of Fig. 9.

Although the agreement is not perfect, the result shows that decreasing $B(M1)$ values can also be obtained by assuming a rotational structure with an appropriate coupling of the involved quasiparticle states. The assumed structure would have negative parity. There is no obvious structure with positive parity by which the observed $B(M1)$ values could be described according to Eq. (4) unless one assumes decreasing K values with increasing spins.

In order to give a final answer to the question on the underlying structure of the $M1$ band in ^{124}Xe, the parity of the band is needed and a comparison to TAC calculations should be performed. Considering the presently available experimental data the proposed rotational structure seems to be reasonable.

Although the $M1$ bands in ^{124}Xe and ^{128}Ba are different, most probably we do not deal with shears bands in both cases, but with rotational bands built on four quasiparticle states, where the spin is gained by increasing collective rotation and not by a successive alignment of the involved quasiparticle spins along a total spin axis I. It can not be excluded, that the involved quasiparticles change their alignments with increasing spins leading to decreasing K values and consequently to decreasing $B(M1)$ values with increasing spin.

VI. *sd*-IBM-1 CALCULATIONS

As already indicated by the GSB $B(E2)$ values shown in Fig. 6, ^{124}Xe seems to be γ soft. To describe this γ softness we used the *sd* version of the interacting boson model (IBM) [3,4]. A previous *sd*-IBM-1 calculation for ^{124}Xe was done in Ref. [2]. We want to test the *sd*-IBM-1 calculation with the new $B(E2)$ values. The IBM-1 has three dynamical limits, the $U(5)$, the $SU(3)$, and the $O(6)$ limit, which can be compared to the geometrical limits of a vibrator, a rigid symmetric rotor, and a γ-soft nucleus, respectively. The Hamiltonian of the extended consistent Q formalism (ECQF) [32,33] of the IBM covers the whole range of structure between these three dynamical symmetry limits by just varying the two structure parameters $(\epsilon'/\kappa, \chi)$:

$$H_{\mathrm{ECQF}} = \kappa\left[\frac{\epsilon'}{\kappa}n_d - Q^\chi \cdot Q^\chi\right]. \qquad (5)$$

The factor κ only sets the absolute energy scale. In terms of s and d bosons the quadrupole operator Q^χ is given by

$$Q^{\mathrm{IBM}} = Q^\chi = [s^\dagger d + d^\dagger s]^{(2)} + \chi[d^\dagger d]^{(2)}. \qquad (6)$$

The quadrupole operator Q^{IBM} is proportional to the $E2$ transition operator $T(E2) = e_B Q^{\mathrm{IBM}}$ by including the effective quadrupole boson charge e_B. Figure 10 shows a fit with this Hamiltonian, using the parameters $\epsilon'/\kappa = -21.6$, $\chi = -0.677$, $\kappa = -31.6$ keV and $e_B = 1.9$ W.u. In this fit the main focus was set on the reproduction of the level energies of the ground state band and the staggering of the quasi-γ band. Compared to the $O(6)$ limit, the experimentally observed staggering of the quasi-γ band in ^{124}Xe is strongly weakened and cannot be reproduced by the calculation using the Hamiltonian given by Eq. (5). Furthermore the calculation overestimates the level energies of the quasi-γ band. To improve the description of the data, we added to the Hamiltonian two new terms, namely the term H^B_{pair} as given in Ref. [34] which takes into account a pairing interaction in order to compress the multiplets according to the quantum number τ (τ compression) and a $(L \cdot L)$ term, as previously used in Ref. [2], to

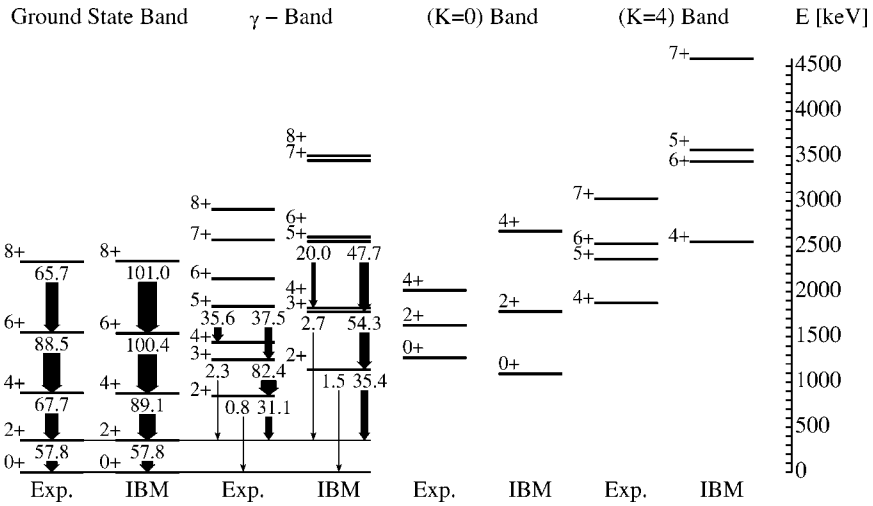

FIG. 10. Low-lying levels and $B(E2)$ values of the ground state band, the quasi-γ band, the $(K=0)$ band and $(K=4)$ band of ^{124}Xe. For a better comparison the experimentally known data for each band are displayed left to the results of the *sd*-IBM-1 calculation, using the ECQF Hamiltonian in Eq. (5). The number above the arrow is the $B(E2)$ value for the corresponding transition in Weiskopf units. The parameters for this calculation are $\epsilon'/k=-21.6$, $\chi=-0.677$, $\kappa=-31.6$ keV, and $e_B=1.9$ W.u.

account for the weakened staggering. The pairing interaction term H^B_{pair} is defined as [34]:

$$H^B_{\text{pair}} = \alpha s^\dagger s + \beta (s^\dagger s)(s^\dagger s), \tag{7}$$

where α and β are parameters. Using the relation $s^\dagger s = N - (d^\dagger d)$ one can write H^B_{pair} as

$$H^B_{\text{pair}} = E_p + \tilde{\epsilon}(d^\dagger d) + \beta (d^\dagger d)(d^\dagger d) = E_p + \tilde{\epsilon} n_d + \beta n_d^2, \tag{8}$$

where E_p is a function of the boson number N and $\tilde{\epsilon}$ is again a parameter. The complete n_d^2-ECQF Hamiltonian used for our calculation is

$$\begin{aligned} H_{n_d^2\text{-ECQF}} &= H_{\text{ECQF}} + H^B_{\text{pair}} + \lambda LL \\ &= \kappa \left(\frac{\epsilon}{\kappa} n_d + Q^\chi Q^\chi + \frac{\lambda}{\kappa} LL + \frac{\beta}{\kappa} n_d^2 \right), \end{aligned} \tag{9}$$

where $\epsilon = \epsilon' + \tilde{\epsilon}$ from Eqs. (8) and (5) and the constant E_p for $N=8$ is omitted. The parameters κ and e_B were fixed to reproduce the energy and the ground state transition strength of the 2_1^+ state. The diagonalization of the Hamiltonian has been done using the code PHINT by Scholten [35].

In Fig. 11 the low-lying energy spectrum of ^{124}Xe is compared to the *sd*-IBM-1 calculation with the n_d^2-ECQF Hamiltonian, using the structure parameters $\epsilon/\kappa=-25.5$ and $\chi=-0.436$, while $\beta/\kappa=2.519$ and $\lambda/\kappa=-0.649$ adjust the level spacing. Further $\kappa=-26.2$ keV and $e_B=1.865$ W.u. were used in this calculation. With these additional terms the weakened staggering in the quasi-γ band is reproduced. The added $(L\cdot L)$ term does not change the wave functions and thus does not influence the transiton strengths. The added pairing interaction H^B_{pair} only slightly changes the $B(E2)$ values, which leads to a good agreement of both calculations with the experimental transition strengths. The disagreement in the energy spacing between the levels of the $(K=0)$ band is a well known problem of *sd*-IBM-1 calculations as well as of other collective models, e.g., the general collective model [36]. Though the τ compression reduces the level spacing in the $(K=0)$ band it also reduces the level energies, so that the 0_2^+ and the 2_3^+ are reproduced worse than in the calculation using the simple ECQF Hamiltonian. Another noticeable difference of both *sd*-IBM-1 calculations is the far better reproduction of the level energies belonging to the $(K=4)$ band, when using the n_d^2-ECQF Hamiltonian.

VII. SUMMARY AND CONCLUSIONS

A recoil distance measurement was performed using the Cologne plunger in combination with the Euroball spectrom-

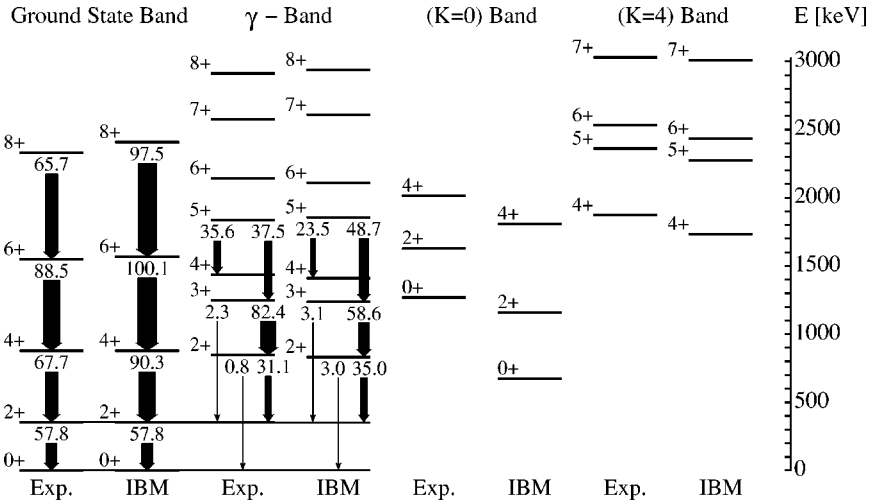

FIG. 11. See the caption of Fig. 10. Unlike Fig. 10, the n_d^2-ECQF Hamiltonian from Eq. (9) was used for this calculation. The parameters are $\epsilon/\kappa=-25.5$, $\chi=-0.436$, $\beta/\kappa=2.519$, $\lambda/\kappa=-0.649$, $\kappa=-26.2$ keV, and $e_B=1.865$ W.u.

eter. Nineteen lifetimes of excited states in ^{124}Xe were derived by means of the DDCM applied on $\gamma\gamma$ coincidence data. The deduced transition probabilities were used to test different theoretical predictions. The $B(E2;0^+\rightarrow 2^+)$ value of ^{124}Xe fits well into the $B(E2;0^+\rightarrow 2^+)$ systematics of the neighboring nuclei and a ground state deformation $\beta = 0.218$ was deduced. A three band mixing calculation for the crossing region of the ground state band with two *s* bands at spins 10−14, shows a good agreement with the experimental data and reveals 70% admixture of $\nu(h_{11/2})^2$ quasiparticle structure to the lowest 10^+ state at 3172 keV, previously assigned to the ground state band. Consequently the 10^+ state at 3503 keV is of 70% ground state band heritage. The deduced $B(M1)$ values of the $M1$ band decrease with increasing spin, which is the expected behavior for magnetic rotation, but can also be described on the basis of a rotational band with negative parity assuming a structure $\pi(h_{11/2})^2 \otimes \nu(h_{11/2}g_{7/2})$ with an effective K value of about $9\hbar$. To give a final answer to the question of the underlying structure of the $M1$ band the parity of the band is required. Two *sd*-IBM-1 calculations with two different Hamiltonians were performed, both showing a good agreement with the experimental $B(E2)$ values and the low energy spectrum. The weakened staggering of the quasi-γ band indeed can only be described by using the n_d^2-ECQF Hamiltonian with a pairing interaction term.

ACKNOWLEDGMENTS

The authors thank S. Heinze, V. Werner, and R. F. Casten for useful discussions. They thank the IReS for their kind hospitality and generous support. One of the authors (D.T.) acknowledges support under Contract No. HPMF-CT-2002-02018. This work was supported by the BMBF under Contract No. 06K167 and under the European Union TMR Programme, Contract No. HPRI-CT-1999-00078.

[1] R. F. Casten *et al.*, Nucl. Phys. **A439**, 289 (1985).
[2] V. Werner *et al.*, Nucl. Phys. **A692**, 451 (2001).
[3] A. Arima and F. Iachello, Phys. Rev. Lett. **35**, 1069 (1975).
[4] F. Iachello and A. Arima, *The Interacting Boson Model* (Cambridge University Press, Cambridge, 1987).
[5] R. Wyss *et al.*, Nucl. Phys. **A505**, 337 (1989).
[6] A. Granderath *et al.*, Nucl. Phys. **A597**, 427 (1996).
[7] I. Schneider *et al.*, Phys. Rev. C **60**, 014312 (1999).
[8] S. Frauendorf, Nucl. Phys. **A557**, 259 (1993).
[9] R. M. Clark *et al.*, Phys. Rev. Lett. **78**, 1868 (1997).
[10] R. M. Clark *et al.*, Phys. Lett. B **440**, 251 (1998).
[11] C. Rossi-Alvarez, Nuovo Cimento Soc. Ital. Fis., A **111A**, 601 (1998).
[12] A. Dewald, in *The '98 Seminar on Nuclear Physics with Radioactive Ion Beam and High Spin Nuclear Structure*, Lanzhou, China, edited by G. Jin, Y. Luo, and W. Zhan (Atomic Energy, Beijing, 1998).
[13] A. Dewald, S. Harissopoulos, and P. von Brentano, Z. Phys. A **334**, 163 (1989).
[14] G. Böhm, A. Dewald, P. Petkov, and P. von Brentano, Nucl. Instrum. Methods Phys. Res. A **329**, 248 (1993).
[15] P. Petkov, Nucl. Instrum. Methods Phys. Res. A **349**, 289 (1994).
[16] A. E. Stuchbery, Nucl. Instrum. Methods Phys. Res. A **385**, 547 (1997).
[17] P. Petkov *et al.*, Nucl. Instrum. Methods Phys. Res. A **431**, 208 (1999).
[18] H. Hanewinkel *et al.*, Phys. Lett. **133**, 9 (1983).
[19] A. Dewald *et al.*, in *Proceedings of XXV Zakopane School of Physics*, Vol. 2, edited by J. Styczeen and Z. Stachura (World Scientific, Singapore, 1990), p. 152.
[20] R. F. Casten, Nucl. Phys. **A443**, 1 (1985).
[21] A. Dewald, Prog. Part. Nucl. Phys. **28**, 409 (1992).
[22] S. Frauendorf, W. Lieberz, P. von Brentano, and A. Gelberg, Phys. Lett. B **274**, 149 (1992).
[23] A. Dewald *et al.*, BgNS Transactions **7**, 81 (2002).
[24] R. M. Clark *et al.*, Nucl. Phys. **A562**, 121 (1993).
[25] G. Baldsiefen *et al.*, Nucl. Phys. **A574**, 521 (1994).
[26] A. O. Macchiavelli *et al.*, Phys. Rev. C **57**, R1073 (1998).
[27] A. O. Macchiavelli *et al.*, Phys. Rev. C **58**, 3746 (1998).
[28] P. Petkov *et al.*, Phys. Rev. C **62**, 014314 (2000).
[29] V. I. Dimitrov, F. Dönau, and S. Frauendorf, Phys. Rev. C **62**, 024315 (2000).
[30] F. Dönau, Nucl. Phys. **A471**, 469 (1987).
[31] T. Lönnroth, S. Vajda, O. C. Kistner, and M. H. Rafailovich, Z. Phys. A **317**, 215 (1984).
[32] D. D. Warner and R. F. Casten, Phys. Rev. Lett. **48**, 1385 (1982).
[33] P. Lipas, P. Toivonen, and D. Warner, Phys. Lett. **155B**, 295 (1985).
[34] X.-W. Pan, T. Otsuka, J.-Q. Chen, and A. Arima, Phys. Lett. B **287**, 1 (1992).
[35] O. Scholten, *The Program-Package Phint*, KVI-63, Groningen.
[36] G. Gneuss and W. Greiner, Nucl. Phys. **A171**, 449 (1971).